AMERICAN SOCIETY FOR MICROBIOLOGY | Applied and Environmental Microbiology®

MICROBIAL ECOLOGY

Investigating the Relationship between Nitrate, Total Dissolved Nitrogen, and Phosphate with Abundance of Pathogenic Vibrios and Harmful Algal Blooms in Rehoboth Bay, Delaware

Detbra Rosales,[a] Ava Ellett,[b] John Jacobs,[b] Gulnihal Ozbay,[c] Salina Parveen,[a] Joseph Pitula[a]

[a]University of Maryland Eastern Shore, Princess Anne, Maryland, USA
[b]USA National Oceanic and Atmospheric Administration, NOS, NCCOS, Marine Spatial Ecology, Oxford, Maryland, USA
[c]Delaware State University, Dover, Delaware, USA

ABSTRACT *Vibrio* spp. and phytoplankton are naturally abundant in marine environments. Recent studies have suggested that the co-occurrence of phytoplankton and the pathogenic bacterium *Vibrio parahaemolyticus* is due to shared ecological factors, such as nutrient requirements. We compared these communities at two locations in the Delaware Inland Bays, representing a site with high anthropogenic inputs (Torquay Canal) and a less developed area (Sloan Cove). In 2017 to 2018, using light microscopy, we were able to identify the presence of many bloom-forming algal species, such as *Karlodinium veneficum*, *Dinophysis acuminata*, *Heterosigma akashiwo*, and *Chattonella subsalsa*. Dinoflagellate biomass was higher at Torquay Canal than that at Sloan Cove. *D. acuminata* and *Chloromorum toxicum* were found only at Torquay Canal and were not observed in Sloan Cove. Most probable number real-time PCR revealed *V. parahaemolyticus* and *Vibrio vulnificus* in environmental samples. The abundance of vibrios and their virulence genes varied between sites, with a significant association between total dissolved nitrogen (TDN), PO_4^-, total dissolved phosphorus (TDP), and pathogenic markers. A generalized linear model revealed that principal component 1 of environmental factors (temperature, dissolved oxygen, salinity, TDN, PO_4^-, TDP, NO_3:NO_2, NO_2^-, and NH_4^+) was the best at detecting total (*tlh*+) *V. parahaemolyticus*, suggesting that they are the prime drivers for the growth and distribution of pathogenic *Vibrio* spp.

IMPORTANCE Vibrio-associated illnesses have been expanding globally over the past several decades (A. Newton, M. Kendall, D. J. Vugia, O. L. Henao, and B. E. Mahon, Clin Infect Dis 54:S391–S395, 2012, https://doi.org/10.1093/cid/cis243). Many studies have linked this expansion with an increase in global temperature (J. Martinez-Urtaza, B. C. John, J. Trinanes, and A. DePaola, Food Res Int 43:10, 2010, https://doi.org/10.1016/j.foodres.2010.04.001; L. Vezzulli, R. R. Colwell, and C. Pruzzo, Microb Ecol 65:817–825, 2013, https://doi.org/10.1007/s00248-012-0163-2; R. N. Paranjpye, W. B. Nilsson, M. Liermann, and E. D. Hilborn, FEMS Microbiol Ecol 91:fiv121, 2015, https://doi.org/10.1093/femsec/fiv121). Temperature and salinity are the two major factors affecting the distribution of *Vibrio* spp. (D. Ceccarelli and R. R. Colwell, Front Microbiol 5:256, 2014, https://doi.org/10.3389/fmicb.2014.00256). However, *Vibrio* sp. abundance can also be affected by nutrient load and marine plankton blooms (V. J. McKenzie and A. R. Townsend, EcoHealth 4:384–396, 2007; L. Vezzulli, C. Pruzzo, A. Huq, and R. R. Colwell, Environ Microbiol Rep 2:27–33, 2010, https://doi.org/10.1111/j.1758-2229.2009.00128.x; S. Liu, Z. Jiang, Y. Deng, Y. Wu, J. Zhang, et al. Microbiologyopen 7:e00600, 2018, https://doi.org/10.1002/mbo3.600). The expansion of *Vibrio* spp. in marine environments calls for a deeper understanding of the biotic and abiotic factors that play a role in their abundance. We observed that pathogenic *Vibrio* spp. were most abundant in areas that favor the proliferation of harmful algal bloom (HAB) species. These results

Editor Charles M. Dozois, INRS

Address correspondence to Joseph Pitula, jspitula@umes.edu.

The authors declare no conflict of interest.

Received 15 March 2022
Accepted 30 May 2022
Published 6 July 2022

can inform managers, researchers, and oyster growers on factors that can influence the growth and distribution of pathogenic *Vibrio* spp. in the Delaware Inland Bays.

KEYWORDS *Vibrio*, Delaware Inland Bays, mid-Atlantic, MPN-PCR, harmful algal blooms

The Delaware Inland Bays (DIBs) are a collection of saltmarshes, tidal flats, oyster reefs, saltwater creeks, and shallow open waters. The DIBs are located in the mid-Atlantic region of the United States, near Rehoboth Beach and Fenwick Island, Delaware. The watershed consists of ~750 square kilometers of land area draining into ~90 square kilometers of bay and tributaries (1). The intensity and duration of harmful algal bloom (HAB) events have been increasing in the United States (2, 3), and a similar pattern has been observed in the DIBs (4–6). These issues have led to concerns regarding potential human exposure to toxins produced by HAB species.

HABs, such as *Karlodinium veneficum* and *Dinophysis* sp., have been detected in tributaries near Little Assawoman Bay, Delaware (6). *Dinophysis* spp. are known to cause diarrhetic shellfish poisoning (DSP) via the production of okadaic acid (OA) and its derivatives, the dinophyistoxins (DTXs), which are lipophilic toxins that accumulate in the fatty tissue of shellfish (7). Blooms of raphidophytes have also been studied extensively in the DIBs and have been responsible for fish mortalities (4, 8). *Heterosigma akashiwo* has been detected regularly in the DIB, and it has the potential to cause sublethal impacts on the eastern oyster (8).

Vibrio spp. are naturally occurring Gram-negative marine bacteria that are found in diverse habitats ranging from coastal to open waters (9). They can survive as free-living organisms or attached to organic particles and biofilms (10). They are able to degrade polymeric substrates, such as chitin, plant/algal polysaccharides, and plastic waste (10). *Vibrio* can colonize and degrade particulate matter and consequently play an important role in chemical transformations, which contributes to cycling of carbon and other nutrients (11). Studies have suggested that organic nutrients that stimulate algal blooms of *Gymnodinium*, *Dinophysis*, and *Ceratium* may be the most significant factor driving interrelationships between *Vibrio* spp. and phytoplankton (12, 13). In the DIB, *Vibrio* spp. have been correlated with particulate matter of >20 μm, which includes phytoplankton, such as diatoms and raphidophytes (14).

A combined abiotic and biotic analysis was performed at two sites in the DIBs, as follows: one, which is known to be impacted negatively by anthropogenic factors (Torquay Canal), and another that is in proximity to a proposed aquaculture site (Sloan Cove). At each location, we (i) analyzed water quality parameters, such as temperature, dissolved oxygen, salinity, and nutrients; (ii) identified and enumerated the HAB species present at both locations; and (iii) examined the levels of total and pathogenic *Vibrio parahaemolyticus* and *Vibrio vulnificus* from collected water. The goal of the study was to determine the most influential factors in the proliferation of two potentially pathogenic *Vibrio* species accounting for environmental factors that may simultaneously influence the development of algal blooms, so as to inform management decisions for aquaculture efforts.

RESULTS

Comparison of environmental parameters between sampling sites, namely, temperature, salinity, dissolved oxygen, and nutrients. Abiotic parameters were measured at two sites in the DIBs (Fig. 1) to establish the relative water quality between sites. On average, the water temperature at Torquay Canal was 24.4°C (range of 12.3 to 31.4°C), and at Sloan Cove, it was 23.5°C (10.4 to 23.5°C). The average salinity at Torquay Canal was 25.6 g/kg (range of 18.1 to 25.6 g/kg), and at Sloan Cove, it was 27.9 g/kg (12.2 to 30.4 g/kg). However, a Mann-Whitney rank sum test revealed that there was not a significant difference in temperature or salinity between sites (see Fig. S1 in the supplemental material).

Water quality at Torquay Canal was degraded compared with that of Sloan Cove (Table 1), with dissolved oxygen averaging 3.9 mg mL^{-1} and 6.3 mg mL^{-1}, respectively. According to a Mann-Whitney rank sum test, there were significant differences in total

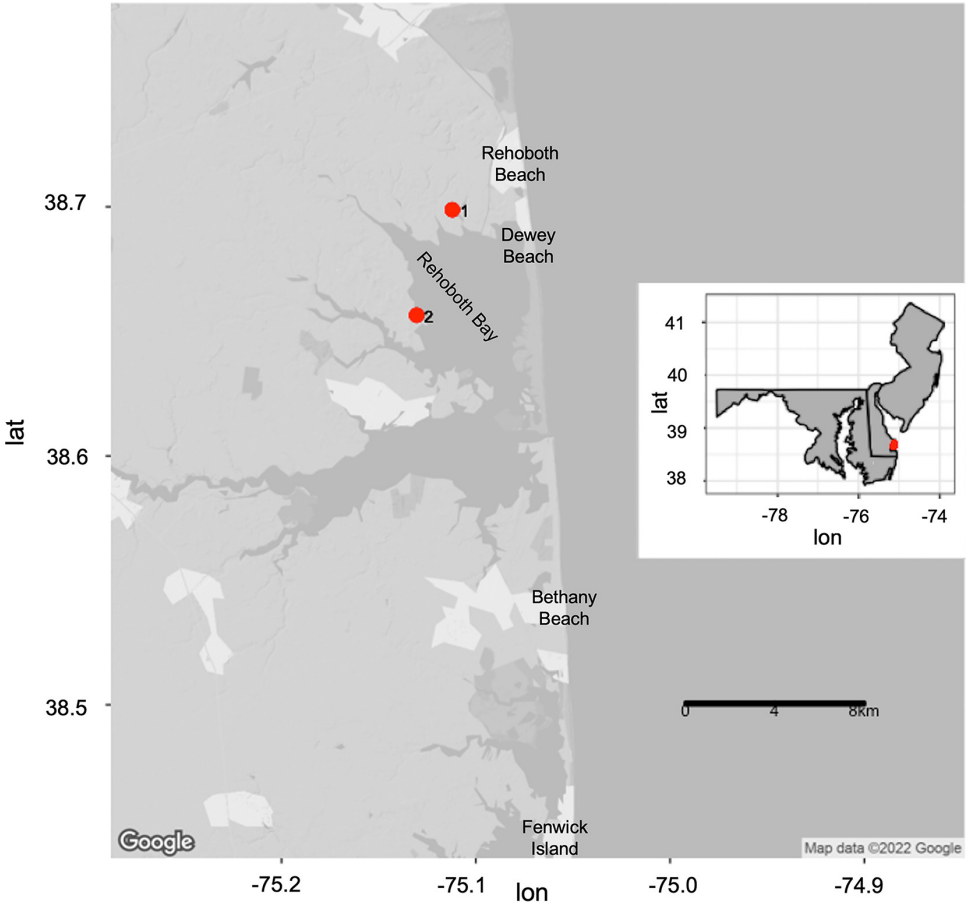

FIG 1 Location of sampling sites in the Delaware Inland Bays. 1, Torquay Canal; 2, Sloan Cove; (The maps were created with ggmaps on R studio [45]).

dissolved phosphorus (TDP), PO_4^{-3}, and total dissolved nitrogen (TDN) between sites ($P < 0.05$). TDP at Torquay Canal averaged 3.48 μM compared with that of 1.46 μM at Sloan Cove, and PO_4^{-3} levels averaged 1.68 μM at Torquay Canal compared with that of 0.81 μM at Sloan Cove, representing an ~2-fold higher concentration of these important phosphorus constituents. There was also a 1.4-fold elevation of TDN at Torquay Canal, which averaged 48.22 μM compared with that of 33.75 μM at Sloan Cove.

Harmful algal community dynamics. As a means of assessing relationships between nutrients and HABs, phytoplankton analyses were performed at each site. The monthly distributions of known HAB species at Torquay Canal and Sloan Cove are shown in Fig. 2 and 3. At Torquay Canal, there was a frequent detection of phytoplankton blooms, including many HAB species, such as *Dinophysis acuminate*, *Chloromorum toxicum*, *Karlodinium veneficum*, and *Heterosigma akashiwo*. *Gymnodinium* spp. (combination of *Gymnodinium auerolum* and *Gymnodinium instratium*), *Scrippsiella trochoidea*, and *Prorocentrum minimum* were also identified routinely. At Sloan Cove, we observed many of the same phytoplankton, although potential toxin-forming species were of lesser prevalence and intensity and *Dinophysis acuminata* and *Chloromorum toxicum* were not detected.

According to the Mann-Whitney rank sum test, there was no significant difference in HAB concentrations between sites and years. However, there was a significant difference in dinoflagellate biomass between sites, with a *P* value of 0.02 (Fig. 4). The total dinoflagellate biomass was 1.4×10^5 μgC·L^{-1} (maximum observed in June 2018) at Torquay Canal and 3.7×10^4 μgC·L^{-1} at Sloan Cove (maximum observed in August 2018). At Torquay Canal, the total *K. veneficum* biomass was 1.6×10^{02} μgC·L^{-1} (maximum observed in May 2017), and it was 133.6 μgC·L^{-1} at Sloan Cove (maximum

TABLE 1 Average distribution of environmental parameters in Rehoboth Bay water samples from 2017 to 2018

	Values by location				
	Sloan Cove		Torquay Canal		
Parameter	Avg	Min/max	Avg	Min/max	*P* value[a]
Dinoflagellate biomass[b]	8.60×10^1	$0/7.20 \times 10^3$	4.60×10^3	$0/2.80 \times 10^3$	**0.04**
K. veneficum biomass[b]	1.40	$0/6.00 \times 10^3$	6.50	0/4.90	0.55
Temp[c]	23.50	10.40/31.60	24.40	12.30/31.40	0.77
Salinity[d]	27.90	12.20/30.40	25.60	18.10/30.90	$\mathbf{1.00 \times 10^{-3}}$
Dissolved oxygen[e]	6.40	3.70/8.80	3.90	1.26/6.19	$\mathbf{1.10 \times 10^{-5}}$
NH_4^{+f}	4.74	0.69/29.30	6.18	0.54/28.20	0.14
NO_3^-:NO_2^{-f}	1.35	0.32/4.99	1.80	0.18/6.06	0.35
NO_2^{-f}	0.40	0.15/1.41	0.43	0.13/1.26	0.16
TDN[f]	33.75	13.1/169.00	48.22	15.1/138.00	$\mathbf{1.68 \times 10^4}$
PO_4^{3-f}	0.81	0.31/1.68	1.68	0.29/7.34	$\mathbf{8.99 \times 10^{-4}}$
TDP[f]	1.46	0.74/3.18	3.48	0.51/17.50	$\mathbf{1.85 \times 10^{-5}}$

[a]Boldface entries indicate significant *P* values.
[b]μgC L^{-1}.
[c]°C.
[d]g/kg.
[e]mg·L^{-1}.
[f]μM.

observed in May 2018). A Mann-Whitney rank sum test found no significant difference in *K. veneficum* biomass (Table 1).

A principal-component analysis (PCA) was also performed to reveal overall relationships within phytoplankton species and environmental factors and between phytoplankton

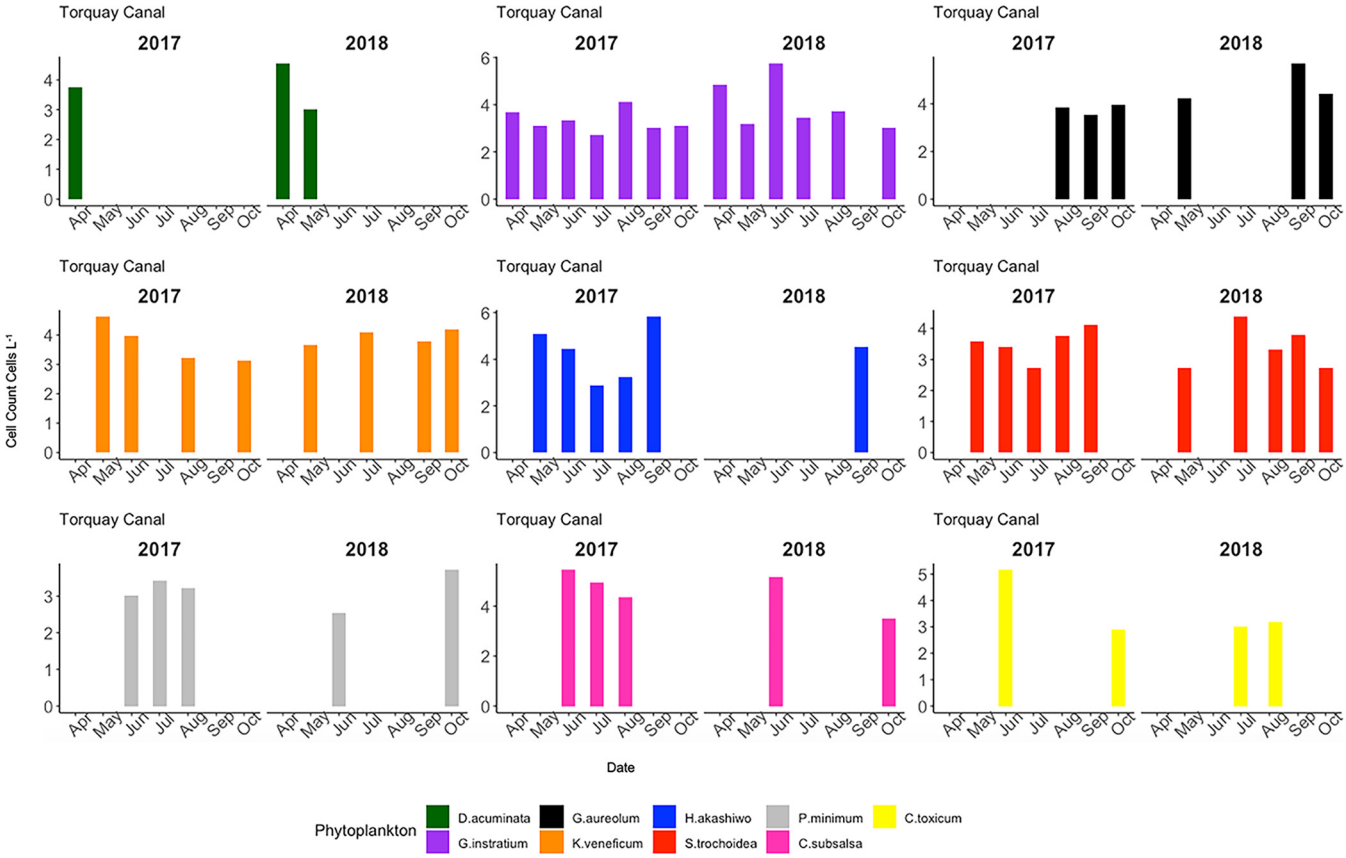

FIG 2 Average distribution of dinoflagellates and raphidophytes in Torquay Canal. The lack of a bar signifies no detection of dinoflagellates or raphidophytes.

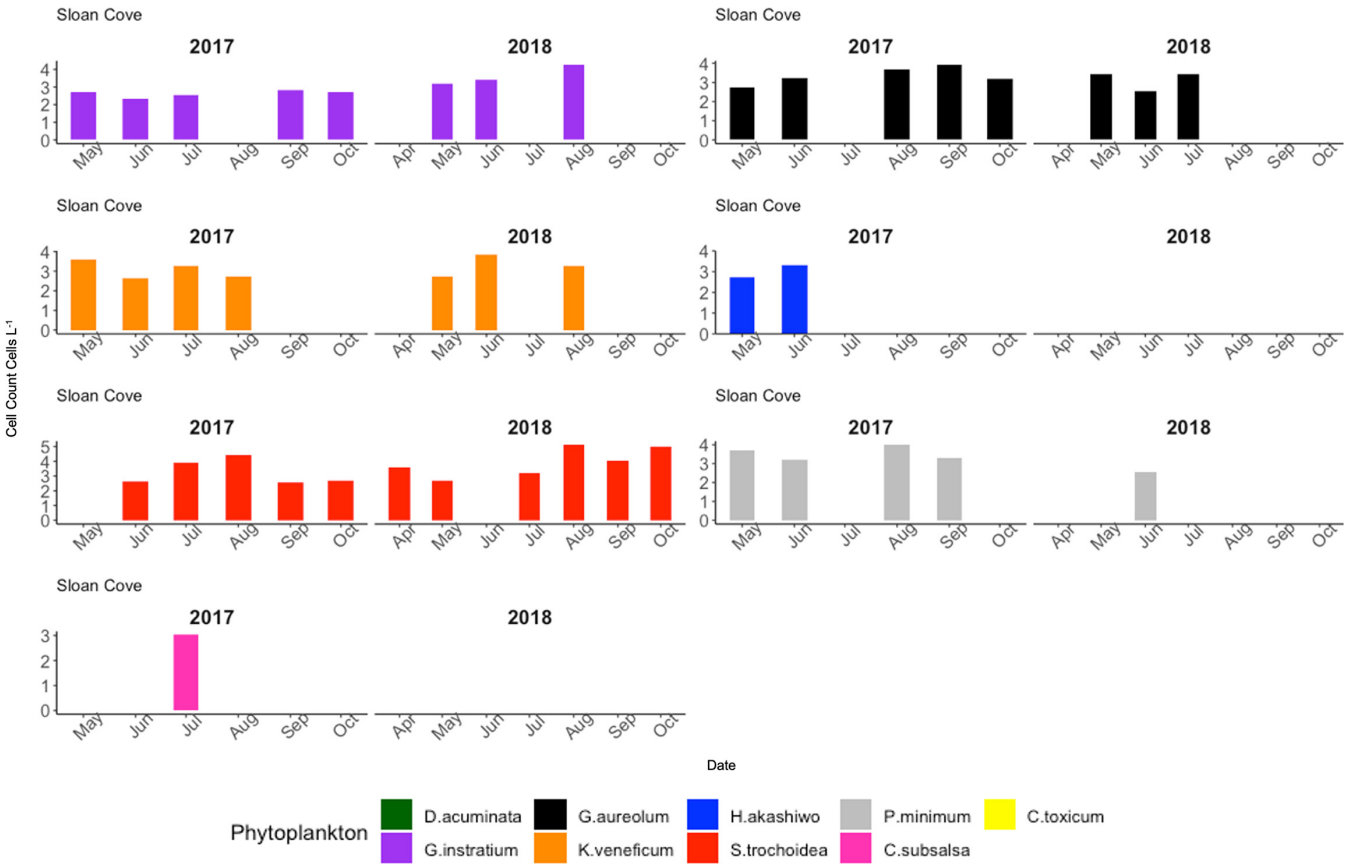

FIG 3 Average distribution of dinoflagellates and raphidophytes in Sloan Cove. The lack of a bar signifies no detection of dinoflagellates or raphidophytes.

groups and environmental variables. An analysis of Torquay Canal and Sloan Cove environmental data showed an association between NO_3:NO_2, NO_2^-, and NH_4^+ and an association between TDN, TDP, and PO_4^{3-} (Fig. 5). Additionally, there was an inverse relationship between low salinity and higher nitrogen constituents. Phytoplankton data showed specific groupings between the following: *Gymnodinium aureolum*, *K. veneficum*, *H. akashiwo*, and *Mesodinium rubrum*; *C. subsalsa*, *C. toxicum*, *P. minimum*, and cryptophytes; and *D. acuminata* and *G. instratium* (Fig. 5). Nutrient and phytoplankton PCA showed that there was an association between cryptophytes, TDP, TDN, and PO_4^{3-} concentrations. *K. veneficum*, *H. akashiwo*, and *G. aureolum* also were associated with *M. rubrum* concentrations (see Fig. S2 in the supplemental material).

***V. parahaemolyticus* levels in water.** Thermolabile hemolysin (*tlh*+) *V. parahaemolyticus* was detected in 20/26 (77%) of water samples from Torquay Canal and in 22/29 (76%) water samples from Sloan Cove (Table 2 and 3). *Tlh*+ *V. parahaemolyticus* levels in Torquay Canal and Sloan Cove ranged from 0.97 to 3.04 log most probable number (MPN) mL^{-1}. Pathogenic thermostable direct hemolysin-positive (*tdh*+) *V. parahaemolyticus* was detected in 12/26 (46%) of water samples from Torquay Canal and 5/29 (17%) of water samples from Sloan Cove. *Tdh*+ *V. parahaemolyticus* concentrations in Torquay Canal and Sloan Cove ranged from 0.47 to 1.63 log MPN mL^{-1}. According to a Fisher exact test, Torquay Canal had a statistically significant higher number of *tdh*+ *V. parahaemolyticus* than Sloan Cove with a *P* value of 0.01.

Pathogenic thermostable related hemolysin-positive (*trh*+) *V. parahaemolyticus* was detected in 9/26 (35%) water samples from Torquay Canal and 5/29 (17%) water samples from Sloan Cove. *Trh*+ *V. parahaemolyticus* levels in Torquay Canal and Sloan Cove ranged from 0.47 to 1.36 MPN mL^{-1}. As with *tdh*+ *V. parahaemolyticus*, Torquay Canal was significantly higher in the number of *trh*+-positive *V. parahaemolyticus* compared with Sloan Cove, with a *P* value of 0.02.

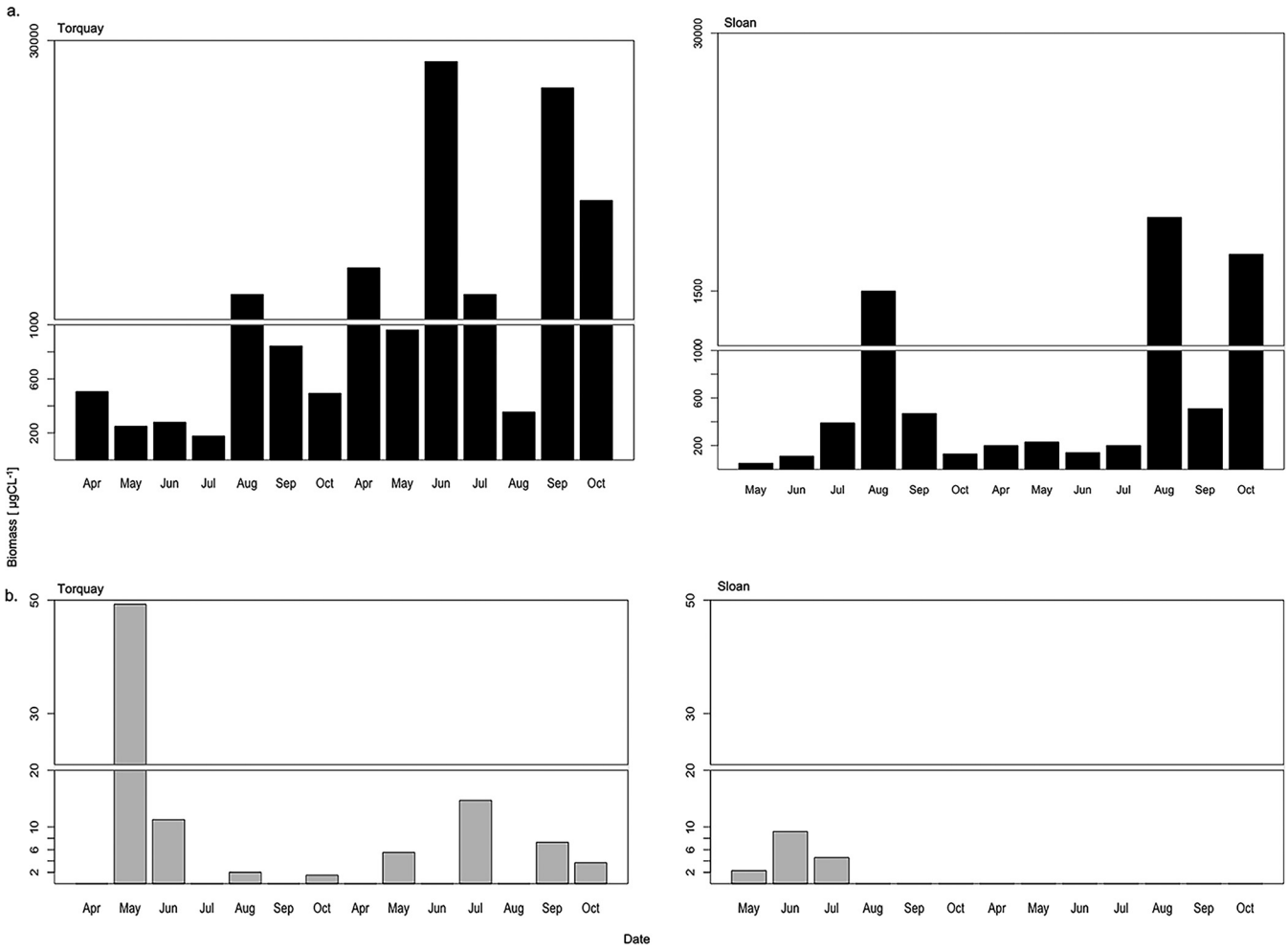

FIG 4 Average biomass of dinoflagellate collected from Sloan Cove and Torquay Canal in 2017 to 2018. (a) Dinoflagellates of >20 μm in size, including *D. acuminata*, *G. aureolum*, *G. instratium*, *S. trochoidea*, and *P. minimum*. (b) Dinoflagellates of <20 μm in size, including *K. veneficum*.

***V. vulnificus* levels in water.** A *V. vulnificus* hemolysin A gene (*VvhA*+) was detected in 15/26 (58%) water samples collected from Torquay Canal and 16/29 (55%) from Sloan Cove. *VvhA*+ *V. vulnificus* levels at Torquay Canal and Sloan Cove ranged from 0.50 to 4.64 log MPNml^{-1}. A *Vibrio*-correlated clinical gene (*VcgC*+) *V. vulnificus* was detected in 12/26 (46%) water samples from Torquay Canal and 6/29 (21%) from Sloan Cove. *VcgC*+ *V. vulnificus* levels in Torquay Canal and Sloan Cove water samples ranged from 0.47 to 1.36 MPN mL^{-1}. *VcgC*+ *V. vulnificus*-positive samples were significantly higher at Torquay Canal than those at Sloan Cove with a *P* value of 0.03.

Comparison between years of *V. parahaemolyticus* and *V. vulnificus*. We also compared the distribution of *V. parahaemolyticus* and *V. vulnificus* in water between 2017 and 2018, pooling data from each site. In 2017, samples were collected only between July and October; thus, we pooled only data for these months for a comparative analysis. In 2017, the highest levels of the *tlh*+ and *tdh*+ *V. parahaemolyticus* were observed (Table 4), and there was a significant difference in the *tlh*+ and *tdh*+ levels between these years (*P* values 0.003 and 0.038, respectively). The highest concentration of *vvhA*+ *V. vulnificus* in water samples was observed in August 2017, and the highest concentration of *vcgC* + *V. vulnificus* was observed in July 2017. However, there was no significant difference between the years (Fig. 6).

Correlation analysis of *Vibrio* spp. and nutrients. A correlation analysis of the 2017 to 2018 Torquay Canal and Sloan Cove nutrient and *Vibrio* data showed that at Torquay Canal, total *tlh* + *V. parahaemolyticus* had a moderate positive correlation

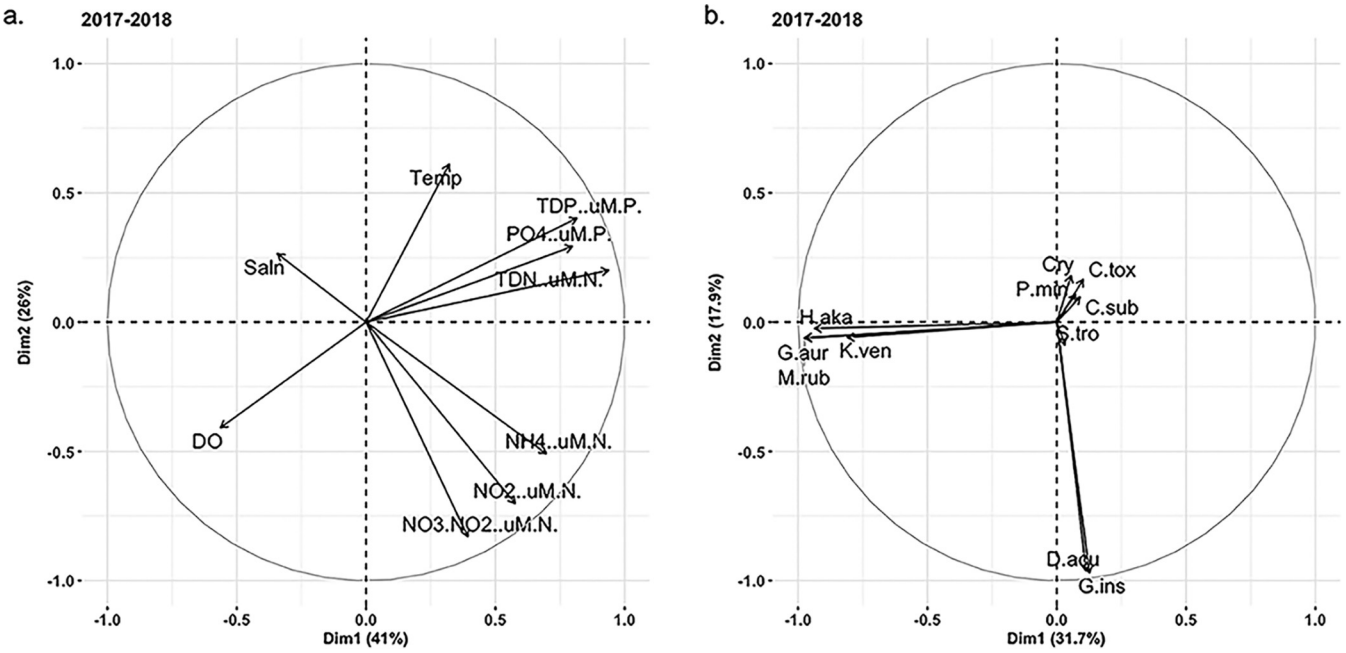

FIG 5 Principal-component analysis of environmental factors and phytoplankton species collected from April to October 2017 to 2018. An abbreviation description is as follows: (a) Saln, salinity; Temp, temperature; DO, dissolved oxygen; (b) P.min, *P. minimum*; D.acu, *D. acuminata*; G.ins, *G. instratium*; G.aur, *G. aureloum*; S.tro, *S. trochoidea*; C.sub, *C. subsalsa*; C.tox, *C. toxicum*; H.aka, *H. akashiwo*; Cry, *Cryptomonads*; K.ven, *K. veneficum*; and M.rub, *M. rubrum*.

with TDP, TDN, and $PO4^{-3}$, with a coefficient value greater than 0.5 and a *P* value of <0.05. *Trh* +*V. parahaemolyticus* had a moderate positive correlation with TDP with a coefficient value greater than 0.5 and a *P* value of <0.05. At Sloan Cove, total *V. vulnificus* (*vvhA*+) had a positive correlation with NO_3:NO_2, with a coefficient value greater than 0.5 and a *P* value of <0.05. All *P* values were corrected using a Benjamini and Hochberg adjustment to avoid false positives.

Modeling the relationship between *Vibrio* spp., HABs, and environmental factors. We used a generalized linear model to determine which explanatory variables best described the detection of *V. parahaemolyticus* (Table 5). Principal component 1 (PC1) of environmental factors (NO_3:NO_2, TDN, and $PO4^{-3}$) contributed the most in

TABLE 2 Distribution of *Vibrio* spp., bloom species, and abiotic parameters in Torquay Canal

Variable	No. positive/total	Percent positive	Min	Max	Avg
V. parahaemolyticus (*tlh*+)[a]	20/26	77	0.97	3.04	1.78
V. parahaemolyticus (*tdh*+)[a]	12/26	46	0.79	1.36	0.54
V. parahaemolyticus (*trh*+)[a]	9/26	35	0.48	1.36	0.388
V. vulnificus (*vvhA*+)[a]	15/26	58	0.50	2.40	1.16
V. vulnificus (*vcgC*+)[a]	12/26	46	0.48	1.36	0.49
Dinophysis acuminata[b]	4/26	15	1.04×10^3	1.04×10^5	4.50×10^3
Gymnodinium spp.[b]	14/26	54	1.04×10^3	2.14×10^5	1.28×10^4
Karlodinium veneficum[b]	4/26	15	2.08×10^3	5.20×10^4	2.99×10^3
Scrippsiella trochoidea[b]	12/26	46	1.04×10^3	6.86×10^4	5.16×10^3
Prorocentrum minimum[b]	11/26	42	1.04×10^3	6.86×10^4	5.43×10^3
Heterosigma akashiwo[b]	5/26	19	1.04×10^3	1.99×10^4	8.52×10^4
Chloromorum toxicum[b]	4/26	15	3.36×10^2	5.65×10^5	1.42×10^5
Temp[c]	na[d]		12.3	31.4	24.4
Salinity[e]	na		18.1	30.9	25.6
Dissolved oxygen[f]	na		1.26	6.19	3.9

[a]log MPN mL^{-1}.
[b]Cells L^{-1}.
[c]°C.
[d]na, not applicable.
[e]g/kg.
[f]mg L^{-1}.

TABLE 3 Distribution of *Vibrio* spp., bloom species, and abiotic parameters in Sloan Cove

Variable	No. positive/total	Percent positive	Min	Max	Avg
V. parahaemolyticus (*tlh*+)[a]	22/29	76	1.36	3.04	1.73
V. parahaemolyticus (*tdh*+)[a]	5/29	17	0.47	1.63	0.20
V. parahaemolyticus (*trh*+)[a]	5/29	17	0.47	1.36	0.15
V. vulnificus (*vvhA*+)[a]	16/29	55	0.97	4.64	0.96
V. vulnificus (*vcgC*+)[a]	6/29	21	0.47	1.36	0.21
Dinophysis acuminata[b]	0/29	0	na	na	na
Gymnodinium spp.[b]	9/29	31	1.04×10^3	7.28×10^3	2.53×10^3
Karlodinium veneficum[b]	7/29	24	1.04×10^3	5.02×10^3	1.11×10^3
Scrippsiella trochoidea[b]	13/29	45	1.04×10^3	8.32×10^3	1.65×10^4
Prorocentrum minimum[b]	7/29	24	1.04×10^3	7.28×10^3	1.42×10^3
Heterosigma akashiwo[b]	3/29	10	2.08×10^3	6.24×10^3	3.47×10^2
Chloromorum toxicum[b]	0/29	0	na	na	na
Temp[c]	na		10.4	31.6	23.5
Salinity[d]	na		12.2	30.4	27.9
Dissolved oxygen[e]	na		3.7	8.8	6.4

[a]log MPN mL^{-1}.
[b]log cells L^{-1}.
[c]°C.
[d]g/kg.
[e]mg L^{-1}.

detecting total (*tlh*+) *V. parahaemolyticus* ($P < 0.05$) (Table 5). *G. instratium* contributed the most in detecting (*tdh*+) *V. parahaemolyticus* ($P < 0.05$) (Table 6). We additionally ran the model using *trh*+, *vvhA*+, and *vcgC*+, but there was no significant relationship discovered (see Fig. S1 to S3 in the supplemental material).

DISCUSSION

Torquay Canal is a dead-end canal, which is common in residential communities close to bays. They are poorly flushed and subject to anthropogenic inputs from homes and other developed areas. Therefore, it was not surprising that its higher nutrient levels and low dissolved oxygen were significantly different from those measured at the well-flushed Sloan Cove. As dead-end canals are also conducive to harmful algal bloom formation (8), these findings were consistent with a higher total dinoflagellate biomass at Torquay Canal than that at Sloan Cove (Fig. 4).

Dinophysis acuminata has been found frequently at Torquay Canal, and favorable growth is associated with elevated nitrogen constituents, particularly NH_4^+ levels (15, 16), consistent with our data (Fig. 2). Additionally, this taxon is also an obligate mixotroph that must sequester chloroplasts from cryptophytes by ingesting ciliates (e.g.,

TABLE 4 Average distribution of *Vibrio* spp., phytoplankton, and abiotic parameters in Rehoboth Bay water samples

	Avg by yr		
Variable	2017	2018	*P* value[a]
V. parahaemolyticus (*tlh*+)[b]	542.82	265.96	**3.00×10^{-3}**
V. parahaemolyticus (*tdh*+)[b]	8.30	2.43	**0.03**
V. parahaemolyticus (*trh*+)[b]	8.17	3.46	0.18
V. vulnificus (*vvhA*+)[b]	188.60	138.68	0.89
V. vulnificus (*vcgC*+)[b]	5.13	6.40	0.47
Phytoplankton[c]	27,630	48,538	0.05
Temp[d]	25.60	21.66	0.07
Salinity[e]	28.22	21.18	**$<1.0 \times 10^{-3}$**
Dissolved oxygen[f]	4.30	3.63	0.83

[a]Boldface entries indicate significant *P* values.
[b]MPN mL^{-1}.
[c]cells L^{-1}.
[d]°C.
[e]g/kg.
[f]mg L^{-1}.

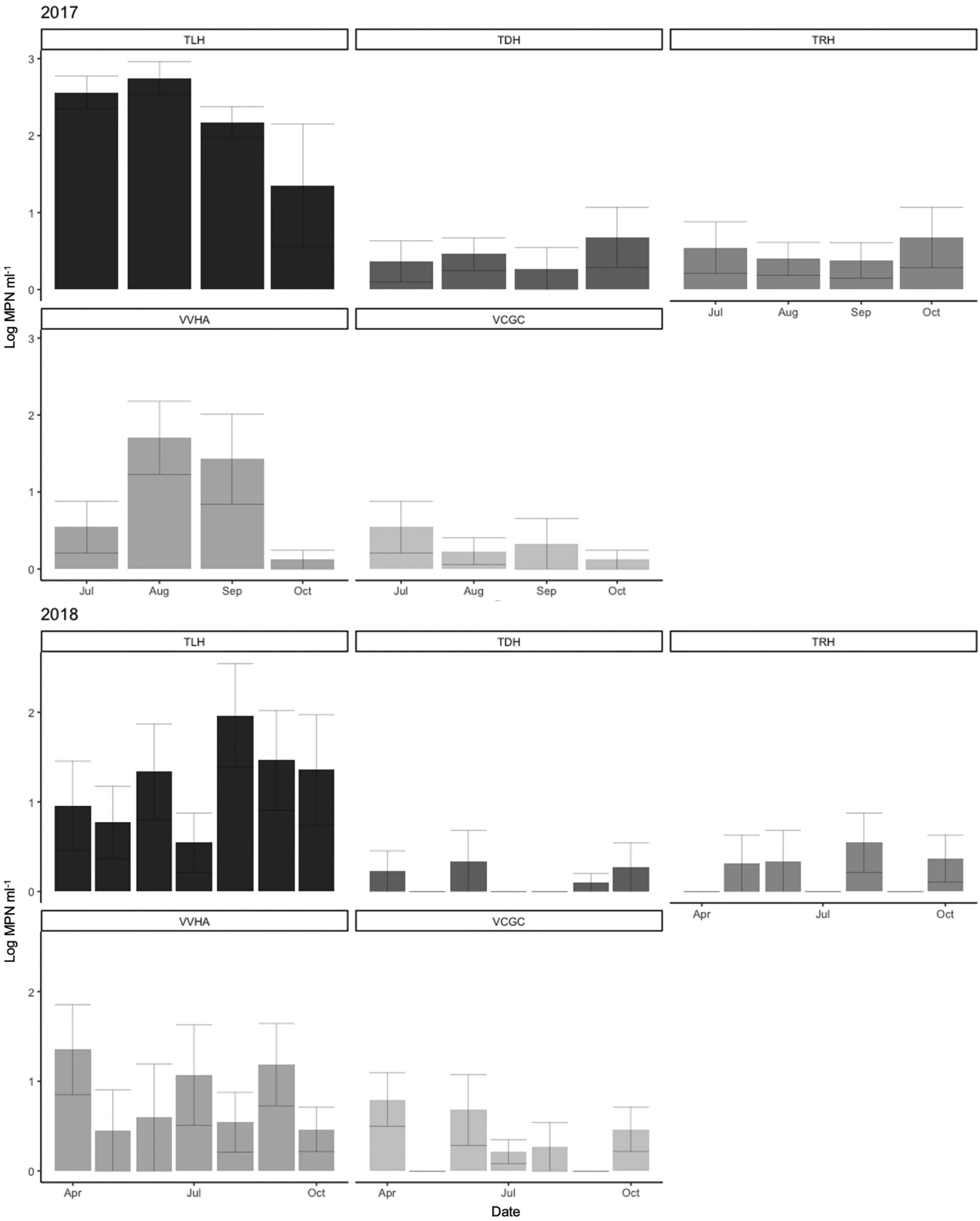

FIG 6 Distribution of *Vibrio* spp. in the Delaware Inland Bays from 2017 to 2018. Shows bar plots of *V. parahaemolyticus* (*tlh*), *V. vulnificus* (*vvha*), pathogenic (*tdh*+ and *trh*+) *V. parahaemolyticus*, and pathogenic (vcgC+) *V. vulnificus*. The bar plots summarize means for *Vibrio* genes. Additionally, standard errors bars were calculated using R studio.

TABLE 5 Model comparison of generalized linear models with *Tlh* as the response variable

Model no.	Explanatory variable	AICc[a]	Delta	wt[b]	RMSE[c]
M6	*Tlh* ~ PC1ENVI[d]	101.1	0.00	0.226	0.968
M100	*Tlh* ~ N023 + PO_4 + TDP	101.3	0.24	0.200	0.898
M28	*Tlh* ~ PC1ENVI + HI[e]	101.9	0.81	0.234	0.943
M97	*Tlh* ~ N02:3	102.1	0.97	0.140	0.982
M29	*Tlh* ~ PC1ENVI + GI[f]	102.4	1.26	0.187	0.949
M27	*Tlh* ~ PC1ENVI + HI + GI	102.9	1.84	0.140	0.919
M1	*Tlh* ~ PC1ENVI + PC2ENVI[g] + PC1HAB[h] + PC2HAB[i]	104.2	3.15	0.073	0.897
M94	*Tlh* ~ Sal	107.0	5.95	0.012	1.05
Null	*Tlh* ~ 1	107.2	6.12	0.016	1.09
M95	*Tlh* ~ Temp	108.8	7.68	0.006	1.08
M31	*Tlh* ~ GI	109.1	8.01	0.005	1.09
M30	*Tlh* ~ HI	109.6	8.52	0.004	1.09

[a]AICc, Akaike's information criterion. A lower AICc indicates a better model.
[b]wt, weight.
[c]RMSE, root-mean-square deviation.
[d]Principal component 1 of environmental variables.
[e]*H. akashiwo*.
[f]*G. instratium*.
[g]Principal component 2 of environmental variables.
[h]Principal component 1 of harmful algal species.
[i]Principal component 2 of harmful algal species.

Mesodinium spp.) that have preyed on cryptophytes (17, 18). Interestingly, we did not observe any *M. rubrum* or cryptophytes in 2018. Either *D. acuminata* ingested all available *M. rubrum* prey prior to our sampling dates in 2018 or *D. acuminata* can obtain chloroplasts from other phytoplankton.

In June and September of 2017 at Torquay Canal, we also observed high levels of *C. subsalsa* and *H. akashiwo* with concentrations ranging from 2.0×10^5 to 6.0×10^5 cells L^{-1}. They are species found commonly in the Delaware Inland Bays (19) and can be both mixotrophic and autotrophic. *C. subsalsa* blooms are known to co-occur with *C. toxicum* in the Delaware Inland Bays (20, 21), as was as also seen in our PCA (Fig. 6).

Sloan Cove did not exhibit as high concentrations of HABs as in Torquay Canal, likely due to the lower nutrient levels. *G. aureolum*, the most commonly reported bloom-forming dinoflagellate in temperate waters (22, 23), was the major species found throughout the 2-year study. HAB species, such as *K. veneficum*, were detected but at low levels. PCA plots revealed associations between *K. veneficum* and *M. rubrum*, which may be reflective of feeding on similar prey items, such as cryptophytes (24–26). In 2017, we detected the presence of both *C. subsalsa* and *H. akashiwo* but not in 2018.

TABLE 6 Model comparison of generalized linear models with *Tdh* as the response variable

Model no.	Explanatory variables	AICc	Delta	wt	RMSE
M36	*Tdh* ~ GI[a]	56.9	0.00	0.339	0.506
M31	*Tdh* ~ PC1ENVI[b] + GI	58.8	1.89	0.132	0.500
M32	*Tdh* ~ PC1ENVI + PC2ENVI[c] + PC1HAB[d] + PC2HAB[e]	59.0	2.03	0.123	0.461
M30	*Tdh* ~ N02:3	59.2	2.32	0.106	0.523
Null3	*Tdh* ~ 1	59.5	2.59	0.093	0.544
M35	*Tdh* ~ HI[f]	61.3	4.37	0.038	0.540
M34	*Tdh* ~ Temp	61.4	4.46	0.036	0.540
M27	*Tdh* ~ PC1ENVI + HI + GI	61.5	4.59	0.012	0.500
M29	*Tdh* ~ PC1ENVI + HI	61.5	4.62	0.034	0.500
M26	*Tdh* ~ PC1ENVI	61.6	4.65	0.033	0.541
M33	*Tdh* ~ Sal	61.8	4.90	0.029	0.541
M28	*Tdh* ~ N023 + PO4 + TDP	62.3	5.36	0.023	0.505

[a]*G. instratium*.
[b]Principal component 1 of environmental variables.
[c]Principal component 2 of environmental variables.
[d]Principal component 1 of harmful algal species.
[e]Principal component 2 of harmful algal species.
[f]*H. akashiwo*.

This finding is likely due to low concentrations of prey items (data not shown) (27, 28). Despite that fewer HAB events occurred in Sloan Cove than those in Torquay Canal, caution should be exercised and routine monitoring continued. Occasional blooms are possible when a "window of opportunity" exists for certain species to outgrow competitors and when there are few zooplankton grazers present (29).

The development of a site-specific *Vibrio* predictive model based on nutrients and resident phytoplankton may be useful for evaluating water quality in oyster aquaculture areas (2). When sampling sites were compared, similar concentrations of total *V. parahaemolyticus* and *V. vulnificus* were recorded, despite differing nutrient and dissolved oxygen concentrations. Whether *V. parahaemolyticus* and *V. vulnificus* prefer different environmental conditions remains unclear. The influence of geographic location is unclear. Some studies suggest that this is the case (30, 31), although we did not observe a significant difference between sites, which is similar to other work (32, 33). The levels of both species during the warmer months, though, were consistent with those reported previously (34–36).

V. parahaemolyticus is a moderately halophilic bacterium (34, 37, 38) and was present at higher levels in the higher salinity year of 2017 (Table 1), although the relationship was weak ($r = 0.032$ and $P = 0.11$) A significant positive association was observed between total *V. parahaemolyticus* and TDN, PO_4^-, and TDP (Fig. S3). Davis et al. also observed a positive association between PO_4^- and *V. parahaemolyticus* in developed areas (34).

Limited work has explored what factors influence the presence of pathogenic strains of *V. parahaemolyticus* and *V. vulnificus*. Previous studies have suggested that chlorophyll *a* levels contribute to higher pathogenic *V. parahaemolyticus* (*tdh*+ and *trh*+) in the water column (31, 39). This suggestion was consistent with our observations, where *trh*+ *V. parahaemolyticus* was present in a higher prevalence and concentrations at Torquay Canal, where there is a significantly higher HAB occurrence and biomass than those at Sloan Cove. Additionally, we observed a positive association between *trh*+ *V. parahaemolyticus* and TDP, which has not been reported previously. According to the generalized linear model (Table 5), PC1 environmental variables that included temperature, dissolved oxygen, salinity, TDN, PO_4^-, TDP, NO_3:NO_2, NO_2^-, and NH_4^+, contributed the most in the detection of total *tlh*+ *V. parahaemolyticus*. *G. instratium* contributed the most in the detection of total *tdh*+ *V. parahaemolyticus*.

Observations from Japan (40) and the Atlantic Coast of the United States (41) have shown that the prevalence of *vcgC*+ *V. vulnificus* can vary depending on the system. A correlation between phosphate and *vcgC*+ *V. vulnificus* has been reported for the Chesapeake Bay (42). We observed a weak correlation between total (v*vha*+) *V. vulnificus* and phytoplankton, which included both dinoflagellates and raphidophytes. This result was unexpected, as prior reports have suggested a strong relationship between total *V. vulnificus* and both nutrients and HABs (43, 44). Thus, any relationship between *V. vulnificus* and phytoplankton might be species specific and be influenced by specific nutrients. Future studies will be necessary to derive these potential interactions.

Future studies in Rehoboth Bay should incorporate chlorophyll *a* data into model development. *Vibrio* spp. are known to bind to the surface of dinoflagellates and raphidophytes (7) and degrade their surface polymers, such as chitin and plant/algal polysaccharides. It is also possible that pathogenic *Vibrio* spp. are more abundant in environments where there is enhanced competition with other marine bacteria and phytoplankton for nutrients. In conclusion, this study sought to characterize the relatedness between *Vibrio* spp. and HABs, as well as determine the influence of nutrients on pathogenic *Vibrio* spp. and HAB abundance in Rehoboth Bay. We discovered that although the total numbers of *Vibrio* spp. are similar between Torquay Canal and Sloan Cove, potentially pathogenic *Vibrio* spp. are more likely to be found at Torquay Canal. Thus, total *Vibrio* counts at a location may not be sufficient for the accurate prediction of pathogenic potential when considering the placement of aquaculture sites.

MATERIALS AND METHODS

Sample collection and phytoplankton enumeration. A total of 55 water samples were collected from Rehoboth Bay in 2017 to 2018, including 29 from Sloan Cove and 26 from Torquay Canal for vibrio and phytoplankton analysis. Surface water samples were collected weekly in 1-L amber glass bottles at Torquay Canal (site 1) and Sloan Cove (site 2). These areas were chosen based on their proximity to oyster aquaculture sites, differences in water quality based on the State of the Delaware Inland Bays report, and accessibility by vehicle (1). Station depth ranged from 5 to 7 feet, and surface temperature, salinity, and dissolved oxygen were collected using a YSI 85 (Yellow Spring Instrument Co., Yellow Springs, OH). At site 1, Torquay Canal water samples were collected from July to October in 2017 and April to October in 2018. At site 2, Sloan Cove water samples were collected from May to October in 2017, and April to October in 2018 (Fig. 1) (45). An additional 50 mL of water was collected from all sites and preserved in Lugol's iodine solution for phytoplankton identification and enumeration via microscopy using a Zeiss IM35 inverted microscope with phase contrast and bright field illumination (46).

The estimated bio-volume of all dinoflagellates was obtained using geometric shape equations from the Baltic Sea environmental proceedings no. 106 and converted to biomass using a conversion factor of 0.760 $pgCm^{-3}$ (cellular carbon) (47). Dinoflagellate biomass as calculated included *D. acuminata*, *G. aureolum*, *G. instratium*, *S. trochoidea*, and *P. minimum*. The biomass of *K. veneficum* was calculated separately because of its small size compared with other dinoflagellates in this study.

Quantification of *V. parahaemolyticus* and *V. vulnificus*. Water samples were also processed for *V. parahaemolyticus* and *V. vulnificus* abundance using the three-tube MPN method following procedures described in reference 48. Totals of 100 mL, 10 mL, 1 mL, 100 μL, 10 μL, and 1 μL of undiluted sample were inoculated in triplicate into 10 mL of alkaline peptone water (APW) broth and incubated overnight at 35°C.

Vibrio sp. analysis using real-time PCR methods targeted the species-specific gene thermolabile hemolysin (*tlh*) to confirm the abundance of *V. parahaemolyticus* and the species-specific gene *Vibrio vulnificus* hemolysin A (*vvha*) to confirm the abundance of *V. vulnificus* in water. Thermostable direct hemolysin (*tdh*) and thermostable related hemolysin (*trh*) were targeted to determine the presence of virulence genes in *V. parahaemolyticus*. Virulence correlated gene (*vcgC*) was targeted to determine the presence of the virulence gene in *V. vulnificus*. Primers, probes, and internal controls were as described previously (49–52).

Real-time PCR was conducted using iTaq universal supermix (Bio-Rad Laboratories, Hercules, CA), as described (51). Real-time PCR cycling was conducted using a Bio-Rad CFX96 real-time system with an initial denaturation/polymerase activation of 95°C for 180 sec, followed by 45 cycles of 95°C for 5 sec, and an annealing temperature of 62°C for 45 sec (53, 54).

Nutrient analysis. A total of 120-mL water samples from both sites were collected for nutrient analysis measurements for 2017 and 2018. Water samples were filtered through a Millipore 0.2-μm mixed cellulose ester membrane, and filtrates were stored at –80°C. Concentrations of total dissolved nitrogen (TDN), total dissolved phosphorus (TDP), nitrate/nitrite (NO_3:NO_2), nitrite (NO_2-), ammonium (NH_4^+), and ortho-phosphate (PO_4^{3-}) were analyzed by the Horn Point Analytical Lab in Cambridge, Maryland, using a Technicon autoanalyzer II and NAP software (55, 56).

Statistical analysis. All *Vibrio* sp. and harmful algal counts were log transformed, and the differences between HABs, *Vibrio* spp., nutrients, biomass, and environmental parameters were evaluated using a Mann-Whitney rank sum test. A Fisher exact test was used to determine if there was a difference in the number of occurrences for and HABs at each site. The Ggplot2 package in R studio was used to generate a visual representation of the distribution of HABs, *Vibrio* spp., and environmental parameters. A Spearman correlation test and a Benjamini and Hochberg *P* value adjustment were used to assess the association between *Vibrio* spp., nutrients, HABs, and environmental parameters. Correlograms were generated using the Corrgram software package in R. Harmful algal species were transformed using Hellinger, and environmental variables were standardized using Z-scoring for principal component analysis (PCA). A visual representation of PCA was used to determine the relationship between environmental factors and to narrow down specific groups of harmful algal species to use in our model. For HAB PCA, *Chloromorum toxicum*, *Scrippsiella* sp., and *Gymnodinium instratium* contributed over 14% in PCA1 and *Karlodinium veneficum* and *Heterosigma akashiwo* contributed over 25% in PCA2. For Environmental PCA, PO_4^{-3}, TDP, and TDN contributed over 18% in PCA1, and NO_2^- and NO_3:NO_2 contributed over 20% in PCA2.

A generalized linear model was used to describe the relatedness between *Vibrio* spp., environmental variables, and harmful algal species. To simplify the model, principal component 1 of environmental variables was used in the model instead of each individual variable. *H. akashiwo* and *Gyrodinium instriatum* were chosen as representatives for the groups that were formed in the PCA plots because these two species were found regularly. MuMIn package in R was used to calculate Akaike information criterion (AICc) to rank the models. The response variable is *tlh* + *V. parahaemolyticus*, and the fixed variables were principal component 1 of environmental variables, principal component 2 of environmental variables, principal component 1 of harmful algal species, principal component 2 of harmful algal species, and *H. akashiwo* and *G. instratium* concentrations. Models included both abiotic and biotic variables. All analyses were conducted using R studio 3.3.0 (57).

SUPPLEMENTAL MATERIAL

Supplemental material is available online only.

SUPPLEMENTAL FILE 1, PDF file, 0.5 MB.

ACKNOWLEDGMENTS

This work was supported by the NOAA Educational Partnership Program with Minority-Serving Institution (EPP/MSI) (award no. NA16SEC481007) and Technical Advisory Board, NOAA Living Marine Resources Cooperative Science Center (award no. 18-06).

We thank Center for Inland Bays, Bob Collins, and Mike Bott for providing us with oysters. Thanks to Ed Whereat and Jennifer Wolny for introducing us to Torquay Canal and providing their expertise in phytoplankton identification. Thanks to Joan Meredith for training and guiding us through the most probable number process. Thanks to Diane Stoecker for suggesting and helping us with biomass calculations. Thanks to Greg Doucette for reviewing our manuscript and providing us with helpful feedback. Thanks also to the directors of Camp Arrowhead, Delaware, for giving us access to their dock.

REFERENCES

1. Center for the Inland Bays. 2011. State of the Delaware Inland Bays. https://www.inlandbays.org/wp-content/documents/2011-state-of-the-bays.pdf.
2. Paranjpye RN, Nilsson WB, Liermann M, Hilborn ED, George BJ, Li Q, Bill BD, Trainer VL, Strom MS, Sandifer PA. 2015. Environmental influences on the seasonal distribution of Vibrio parahaemolyticus in the Pacific Northwest of the USA. FEMS Microbiol Ecol 91:fiv121. https://doi.org/10.1093/femsec/fiv121.
3. Trainer VL, Moore L, Bill BD, Adams NG, Harrington N, Borchert J, da Silva DA, Eberhart BT. 2013. Diarrhetic shellfish toxins and other lipophilic toxins of human health concern in Washington State. Mar Drugs 11:1815–1835. https://doi.org/10.3390/md11061815.
4. Handy SM, Demir E, Hutchins DA, Portune KJ, Whereat EB, Hare CE, Rose JM, Warner M, Farestad M, Cary SC, Coyne KJ. 2008. Using quantitative real-time PCR to study competition and community dynamics among Delaware Inland Bays harmful algae in field and laboratory studies. Harmful Algae 7:599–613. https://doi.org/10.1016/j.hal.2007.12.018.
5. Whereat E. 2015. Dinophysis acuminata in Delaware's Inland Bays and coastal waters 2001–2015 [PowerPoint Slides]. https://www.inlandbays.org/wp-content/uploads/Dinophysis-in-DE-2001-2015-Whereat-STAC-DEC-2015.pdf.
6. FAO. 2004. Marine biotoxins. Food and nutrition paper. FAO, Rome, Italy.
7. Bourdelais AJ, Tomas CR, Naar J, Kubanek J, Baden DG. 2002. New fish-killing alga in coastal Delaware produces neurotoxins. Environ Health Perspect 110:465–470. https://doi.org/10.1289/ehp.02110465.
8. Maxted RJ, Eskin AR, Weisberg BS, Kutz WF, Chaillou CJ. 1997. The ecological condition of dead-end canals of the Delaware and Maryland Coastal Bays. Estuaries 20:319–327. https://doi.org/10.2307/1352347.
9. Ceccarelli D, Colwell RR. 2014. Vibrio ecology, pathogenesis, and evolution. Front Microbiol 5:256. https://doi.org/10.3389/fmicb.2014.00256.
10. Takemura AF, Chien DM, Polz MF. 2014. Associations and dynamics of Vibrionaceae in the environment, from the genus to the population level. Front Microbiol 5:38. https://doi.org/10.3389/fmicb.2014.00038.
11. Dang H, Lovell RC. 2016. Microbial surface colonization and biofilm development in marine environments. Microbiol Mol Biol Rev 80:91–138. https://doi.org/10.1128/MMBR.00037-15.
12. Zhang X, Lin H, Wang X, Austin B. 2018. Significance of Vibrio species in the marine organic carbon cycle—a review. Sci China Earth Sci 61:1357–1368. https://doi.org/10.1007/s11430-017-9229-x.
13. Eiler A, Johansson M, Bertilsson S. 2006. Environmental influences on Vibrio populations in northern temperate and boreal coastal waters (Baltic and Skagerrak Seas). Appl Environ Microbiol 72:6004–6011. https://doi.org/10.1128/AEM.00917-06.
14. Main CR, Salvitti LR, Whereat EB, Coyne KJ. 2015. Community-level and species-specific associations between phytoplankton and particle-associated vibrio species in Delawaress Inland Bays. Appl Environ Microbiol 81:5703–5713. https://doi.org/10.1128/AEM.00580-15.
15. Mohamed ZA, Al-Shehri AM. 2011. Occurrence and germination of dinoflagellate cysts in surface sediments from the Red Sea off the coasts of Saudi Arabia. Oceanologia 53:121–136. https://doi.org/10.5697/oc.53-1.121.
16. Hattenrath-Lehmann TK, Marcoval MA, Mittlesdorf H, Goleski JA, Wang Z, Haynes B, Morton SL, Gobler CJ. 2015. Nitrogenous nutrients promote the growth and toxicity of Dinophysis acuminata during estuarine bloom events. PLoS One 10:e0124148. https://doi.org/10.1371/journal.pone.0124148.
17. Stoecker DK, Hansen PJ, Caron DA, Mitra A. 2017. Mixotrophy in the marine plankton. Annu Rev Mar Sci 9:311–335. https://doi.org/10.1146/annurev-marine-010816-060617.
18. Kim M, Nam SW, Shin W, Coats DW, Park MG. 2012. *Dinophysis caudata* (Dinophyceae) sequesters and retains plastids from the mixotrophic ciliate prey *Mesodinium rubrum*. J Phycol 48:569–579. https://doi.org/10.1111/j.1529-8817.2012.01150.x.
19. Zhang Y, Fu F-x, Whereat EB, Coyne KJ, Hutchins D. 2006. Bottom-up controls on a mixed-species HAB assemblage: a comparison of sympatric Chattonella subsalsa and Heterosigma akashiwo (Raphidophyceae) isolates from the Delaware Inland Bays, USA. Harmful Algae 5:310–320. https://doi.org/10.1016/j.hal.2005.09.001.
20. Whereat DE. 2003. Phytoplankton monitoring report. *In* Volunteer phytoplankton monitoring program. University of Delaware, Lewes, DE.
21. Handy MS, Hutchins AD, Cary SC, Coyne JK. 2006. Simultaneous enumeration of multiple raphidophyte species by quantitative real-time PCR: capabilities and limitations. Limnol Oceanogr Methods 4:193–204. https://doi.org/10.4319/lom.2006.4.193.
22. Jeong HJ. 2011. Mixotrophy in red tide algae raphidophytes. J Eukaryot Microbiol 58:215–222. https://doi.org/10.1111/j.1550-7408.2011.00550.x.
23. Hansen G, Daugbjerg N, Henriksen P. 2003. Comparative study of *Gymnodinium mikimotoi* and *Gymnodinium aureolum*, comb. Nov. (= *Gyrodinium aureolum* based on morphology, pigment composition, and molecular data). J Phycol 36:394–410. https://doi.org/10.1046/j.1529-8817.2000.99172.x.
24. Li A, Stoecker DK, Adolf JE. 1999. Feeding, pigmentation, photosynthesis and growth of the mixotrophic dinoflagellate *Gyrodinium galatheanum*. Aquat Microb Ecol 19:163–176. https://doi.org/10.3354/ame019163.
25. Johnson MD, Stoecker DK, Marshall HG. 2013. Seasonal dynamics of *Mesodinium rubrum* in Chesapeake Bay. J Plankton Res 35:877–893. https://doi.org/10.1093/plankt/fbt028.
26. Johnson MD, Beaudoin JD, Frada JM, Brownlee FE, Stoecker DK. 2018. High grazing rates on cryptophytes algae in Chesapeake Bay. Front Mar Sci 5:1–15. https://doi.org/10.3389/fmars.2018.00241.
27. Handy MS, Coyne JK, Portune JK, Demir E, Doblin AM, Hare EC, Cary SC, Hutchins AD. 2005. Evaluating vertical migration behavior of harmful raphidophytes in the Delaware Inland Bays utilizing quantitative real-time PCR. Aquat Microb Ecol 40:121–132. https://doi.org/10.3354/ame040121.
28. Jeong H, Yoo Y, Kang N, Rho J, Seong K, Park J, Nam G, Yih W. 2010. Ecology of Gymnodinium aureolum. I. Feeding in western Korean waters. Aquat Microb Ecol 59:239–255. https://doi.org/10.3354/ame01394.
29. Stoecker DK, Thessen AE, Gustafson DE. 2008. "Windows of opportunity" for dinoflagellate blooms: reduced microzooplankton net growth coupled to eutrophication. Harmful Algae 8:158–166. https://doi.org/10.1016/j.hal.2008.08.021.
30. Johnson CN, Bowers JC, Griffitt KJ, Molina V, Clostio RW, Pei S, Laws E, Paranjpye RN, Strom MS, Chen A, Hasan NA, Huq A, Noriea NF, Grimes DJ, Colwell RR. 2012. Ecology of Vibrio parahaemolyticus and Vibrio vulnificus in the coastal and estuarine waters of Louisiana, Maryland, Mississippi, and Washington (United States). Appl Environ Microbiol 78:7249–7257. https://doi.org/10.1128/AEM.01296-12.
31. Johnson CN, Flowers AR, Noriea NF, Zimmerman AM, Bowers JC, DePaola A, Grimes DJ. 2010. Relationships between environmental factors and pathogenic Vibrios in the Northern Gulf of Mexico. Appl Environ Microbiol 76:7076–7084. https://doi.org/10.1128/AEM.00697-10.

32. Froelich BA, Phippen B, Fowler P, Noble RT, Oliver JD. 2017. Differences in abundances of total Vibrio spp., V. vulnificus, and V. parahaemolyticus in clams and oysters in North Carolina. Appl Environ Microbiol 83:e02265-16. https://doi.org/10.1128/AEM.02265-16.
33. Fukushima H, Seki R. 2004. Ecology of Vibrio vulnificus and Vibrio parahaemolyticus in brackish environments of the Sada River in Shimane Prefecture, Japan. FEMS Microbiol Ecol 48:221–229. https://doi.org/10.1016/j.femsec.2004.01.009.
34. Davis BJK, Jacobs JM, Davis MF, Schwab KJ, DePaola A, Curriero FC. 2017. Environmental Determinants of Vibrio parahaemolyticus in the Chesapeake Bay. Appl Environ Microbiol 83:e01147-17. https://doi.org/10.1128/AEM.01147-17.
35. Urquhart EA, Jones SH, Yu JW, Schuster BM, Marcinkiewicz AL, Whistler CA, Cooper VS. 2016. Environmental conditions associated with elevated Vibrio parahaemolyticus concentrations in Great Bay Estuary, New Hampshire. PLoS One 11:e0155018. https://doi.org/10.1371/journal.pone.0155018.
36. Sobrinho PS, Destro MT, Franco BD, Landgraf M. 2010. Correlation between environmental factors and prevalence of Vibrio parahaemolyticus in oysters harvested in the southern coastal area of Sao Paulo State, Brazil. Appl Environ Microbiol 76:1290–1293. https://doi.org/10.1128/AEM.00861-09.
37. Parveen S, Jacobs J, Ozbay G, Chintapenta LK, Almuhaideb E, Meredith J, Ossai S, Abbott A, Grant A, Brohawn K, Chigbu P, Richards GP. 2020. Seasonal and geographical differences in total and pathogenic Vibrio parahaemolyticus and Vibrio vulnificus levels in seawater and oysters from the Delaware and Chesapeake Bays determined using several methods. Appl Environ Microbiol 86:e01581-20. https://doi.org/10.1128/AEM.01581-20.
38. Hartwick MA, Urquhart EA, Whistler CA, Cooper VS, Naumova EN, Jones SH. 2019. Forecasting seasonal vibrio parahaemolyticus concentrations in New England shellfish. Int J Environ Res Public Health 16:4341. https://doi.org/10.3390/ijerph16224341.
39. Parveen S, Hettiarachchi KA, Bowers JC, Jones JL, Tamplin ML, McKay R, Beatty W, Brohawn K, Dasilva LV, Depaola A. 2008. Seasonal distribution of total and pathogenic Vibrio parahaemolyticus in Chesapeake Bay oysters and waters. Int J Food Microbiol 128:354–361. https://doi.org/10.1016/j.ijfoodmicro.2008.09.019.
40. Yokochi N, Tanaka S, Matsumoto K, Oishi H, Tashiro Y, Yoshikane Y, Nakashima M, Kanda K, Kobayashi G. 2013. Distribution of virulence markers among Vibrio vulnificus isolates of clinical and environmental origin and regional characteristics in Japan. PLoS One 8:e55219. https://doi.org/10.1371/journal.pone.0055219.
41. Warner E, Oliver JD. 2008. Population structures of two genotypes of Vibrio vulnificus in oysters (Crassostrea virginica) and seawater. Appl Environ Microbiol 74:80–85. https://doi.org/10.1128/AEM.01434-07.
42. Jacobs JM, Rhodes M, Brown CW, Hood RR, Leight A, Long W, Wood R. 2014. Modeling and forecasting the distribution of Vibrio vulnificus in Chesapeake Bay. J Appl Microbiol 117:1312–1327. https://doi.org/10.1111/jam.12624.
43. Lassus P, Chomerat N, Hess P, Nezan E. 2016. Toxic and harmful microalgae of the world ocean. UNESDOC, Copenhagen, Denmark.
44. Greenfield DI, Gooch Moore J, Stewart JR, Hilborn ED, George BJ, Li Q, Dickerson J, Keppler CK, Sandifer PA. 2017. Temporal and environmental factors driving Vibrio vulnificus and V. parahaemolyticus populations and their associations with harmful algal blooms in South Carolina detention ponds and receiving tidal creeks. Geohealth 1:306–317. https://doi.org/10.1002/2017GH000094.
45. Kahle D, Wickham H. 2013. Ggmap: spatial visualization with ggplot2. The R J 5:144–161. https://doi.org/10.32614/RJ-2013-014.
46. Marshall H, Alden R. 1990. A comparison of phytoplankton assemblages and environmental relationships in three estuarine rivers of the lower Chesapeake Bay. Estuaries 13:287–300. https://doi.org/10.2307/1351920.
47. Menden-Deuer S, Lessard EJ. 2000. Carbon to volume relationships for dinoflagellates, diatoms, and other protist plankton. Limnol Oceanogr 45:569–579. https://doi.org/10.4319/lo.2000.45.3.0569.
48. Esteves K, Hervio-Heath D, Mosser T, Rodier C, Tournoud MG, Jumas-Bilak E, Colwell RR, Monfort P. 2015. Rapid proliferation of Vibrio parahaemolyticus, Vibrio vulnificus, and Vibrio cholerae during freshwater flash floods in French Mediterranean coastal lagoons. Appl Environ Microbiol 81:7600–7609. https://doi.org/10.1128/AEM.01848-15.
49. Baker-Austin C, Stockley L, Rangdale R, Martinez-Urtaza J. 2010. Environmental occurrence and clinical impact of Vibrio vulnificus and Vibrio parahaemolyticus: a European perspective. Environ Microbiol Rep 2:7–18. https://doi.org/10.1111/j.1758-2229.2009.00096.x.
50. Nordstrom JL, Vickery MC, Blackstone GM, Murray SL, DePaola A. 2007. Development of a multiplex real-time PCR assay with an internal amplification control for the detection of total and pathogenic Vibrio parahaemolyticus bacteria in oysters. Appl Environ Microbiol 73:5840–5847. https://doi.org/10.1128/AEM.00460-07.
51. Panicker G, Bej AK. 2005. Real-time PCR detection of Vibrio vulnificus in oysters: comparison of oligonucleotide primers and probes targeting vvhA. Appl Environ Microbiol 71:5702–5709. https://doi.org/10.1128/AEM.71.10.5702-5709.2005.
52. Blodget R. 2010. BAM appendix 2: most probable number from serial dilutions. https://www.fda.gov/food/laboratory-methods-food/bam-appendix-2-most-probable-number-serial-dilutions.
53. Panicker G, Call DR, Krug MJ, Bej AK. 2004. Detection of pathogenic *Vibrio* spp.in shellfish by using multiplex PCR and DNA microarrays. Appl Environ Microbiol 70:7436–7444. https://doi.org/10.1128/AEM.70.12.7436-7444.2004.
54. Lane L, Rhoades S, Thomas C, Van Heukelem L. 2000. Analytical services laboratory-standard operating procedures. Technical report number TS-264–00. Horn Point Laboratory, University of Maryland Center for Environmental Science, Cambridge, MD.
55. Elmahdi S, Parveen S, Ossai S, DaSilva LV, Jahncke M, Bowers J, Jacobs J. 2018. Vibrio parahaemolyticus and Vibrio vulnificus recovered from oysters during an oyster relay study. Appl Environ Microbiol 84:e01790-17. https://doi.org/10.1128/AEM.01790-17.
56. Keefe CW, Blodniker LK, Boynton RW, Clark CA, Frank MJ, Kaumeyer LN, Weir WM, Wood VK, Zimmerman FC. 2004. Nutrient analytical service laboratory standard operating procedures. Technical report number SS-80–04-CBL. Chesapeake Biological Laboratory, University of Maryland Center for Environmental Science, Cambridge, MD.
57. R Studio Team 2015. RStudio: integrated development for R. RStudio, Inc., Boston, MA. http://www.rstudio.com/.